Decoding aggregated profiles using dynamic calibration of machine vibration data.

Vladimir N. Kulikov [†]
Wicher P. Bergsma[‡]

01.12.2004

Abstract: We investigate the feasibility of using vibration measurements for the ultimate goals of online monitoring of machine performance (rather than failure) and the assessment of the remaining life-time of components. For these purposes, experimental data from a photocopying machine are used. Salient features in the measurements, such as the maximum vibration induced by the stapler, are extracted from the experimental data and dynamic calibration methods are proposed for recovering internal machine settings from these features. It is shown that internal machine parameters which are difficult to measure externally can indeed be recovered from the vibration data with a very high success rate. This opens up the possibility for online monitoring of machine performance by dynamic calibration of the aggregated profile of the machine's vibrations.

Keywords: signature analysis, forward and reverse calibration, dynamic calibration, vibration data, photocopying machines, online monitoring, machine performance, prediction of remaining lifetime of components, principal component analysis

[†]EURANDOM, P.O. Box 513 - 5600 MB Eindhoven, the Netherlands, kulikov 'at' eurandom.nl
[‡]EURANDOM, P.O. Box 513 - 5600 MB Eindhoven, the Netherlands, bergsma 'at' eurandom.nl

1 Introduction

The present paper is inspired by two current trends in industry. Firstly, driven by environmental issues, new EU legislation, to be effective from 2006, will make manufacturers responsible for the entire life cycle of certain products, including their disposal. Moreover, the lifetime of a commercial product is nowadays much shorter than the actual lifetime of hardware. For example, newly designed photocopying machines are functioning using the same electric motors but new software. Re-use of modules and components is therefore becoming increasingly important, and methods are needed to estimate their expected remaining lifetime. Secondly, as businesses are becoming more reliant on technology, the cost of machine failures increases dramatically. On-line monitoring of machines, allowing replacement of parts *before* failure, is therefore a potentially important method of improving customer service. Flextronics, producer of photocopying machines, has initiated a joint project with Eindhoven University of Technology and EURANDOM, which is part of the programme *Economy, Ecology and Technology* (EET, see www.eet.nl/english/), organized by the Dutch Ministry of Economic Affairs, the Dutch Ministry of Education, Culture and Science, and the Dutch Ministry of Housing, Spatial Planning and the Environment, in order to investigate the possibility of meeting these goals. Several experiments have been carried out for assessing the feasibility of on-line monitoring and re-use of components. In one of these experiments, carried out in 2002, the vibrations produced by a copying machine during operation have been measured, while varying settings of internal machine parameters. The internal parameters are all parameters of the machine varied during the experiment. Using vibration signals in this respect is highly promising, as is demonstrated e.g. by [1], [2], [3], [4]. Some of the internal parameters may be indicative of the performance of the photocopying machine, whereas other parameters are nuisance parameters.

The specific question addressed in this paper is whether the internal state of the machine can be determined using dynamic calibration of the aggregated profile of the machine's vibrations. Calibration is a technique for recovering difficult to measure "internal" parameters of a system from easily measurable "external" parameters. Normally, calibration is applied to static data, for example, in chemical engineering, where it is very helpful in the determination of the ion concentration in a solution. Ion concentration is difficult to measure directly but can be determined knowing the electric resistance of the solution. Additionally, calibration is often applied during spectral analysis. This paper extends calibration techniques to *signals*, that is, to the time domain. We will refer to this as *dynamic* calibration. Furthermore, this paper demonstrates that calibration techniques can, in principle, be used for the online monitoring of machine *performance* (rather than failure) and assessment of the remaining life-time of components.

Since the vibration signal contain a huge number of measurements, and since neighboring measurements are highly dependent, it has to be compressed to a few salient parameters, that is, a parsimonious representation of the signal has to be found. We propose such a compression and apply two methods of calibration to the compressed signals: (i) *Forward calibration* is the most commonly used one and is based on regression of internal parameters on external ones, and (ii) *Reverse calibration* is based on regression of external parameters on internal parameters and a subsequent inversion of these regressions. We also consider a situation when it is known in advance what the possible values of the initial parameters are and when the set of all possible values is discrete. This may be helpful not only in order to assess accuracy of the method, but also for the case when all normal and critical values of

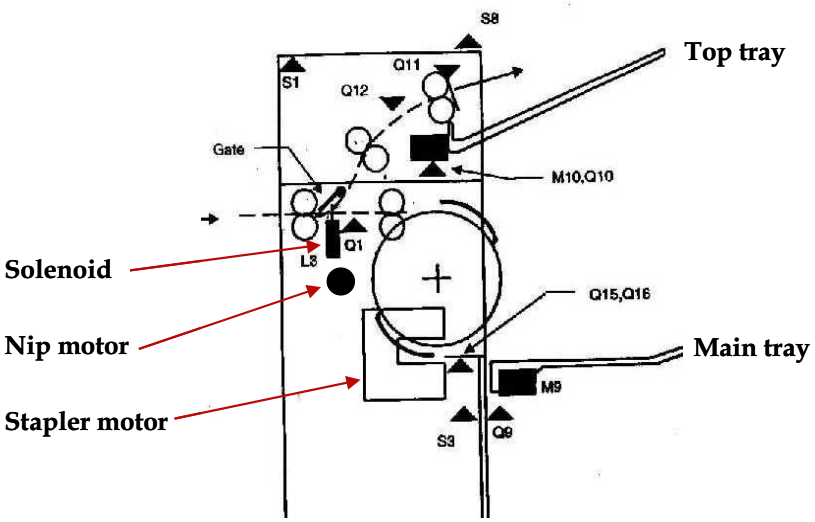

Figure 1: Three parts of the finisher module involved in the experiment.

the parameters are related to some of the most characteristic values or when some values are physically not possible.

Applied to the experimental data, reverse calibration proves to be the most accurate and stable. It not only requires a smaller training set in order to reach the same accuracy level but also for a smaller training set it is able to account for the greater part of the information contained in the data.

In Section 2, the experimental setup is described and the internal parameters to be recovered by calibration are given. In Section 3, the focus of the analyses of this paper, namely the stapling operation, is described and the external parameters obtained from the vibration signals during stapling are defined. In Section 4, two different methods for calibration are described, and their relative merits are assessed. A conclusion and discussion is given in Section 5.

2 Description of the experiment and measurements

In this section a summary is given of the experiment carried out by Flextronics and PD&E. A more extensive description can be found in [5]. The experiment concerns the finisher module of a photocopying machine, and measurements were done during the processing of sheets of paper. For efficiency reasons, a single machine was tested during and the experiment lasted for two days. It should not be problematic to generalize from this machine to other machines of the same type, since experience from other experiments indicates that the between machine variation is small with respect to the present measurements. Furthermore, the aim of the present paper is to provide a general methodology rather than a detailed analysis of the copying machine itself. Three parts of the finisher module were of interest in the experiment: the solenoid, the stapler motor, and the nip motor (see Figure 1). The stapler motor stitches three staples in each piece of paper, the nip motor regulates the paper transport process and the solenoid decides whether the paper goes to main or top tray. There were five time intervals in which the measurements for the motors and the solenoid are taken. A schematic

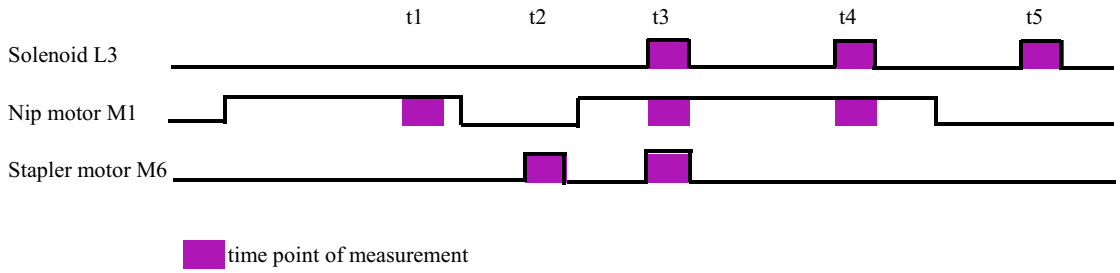

Figure 2: Time sequence of measurements on the parts shown in Figure 1 for one piece of paper.

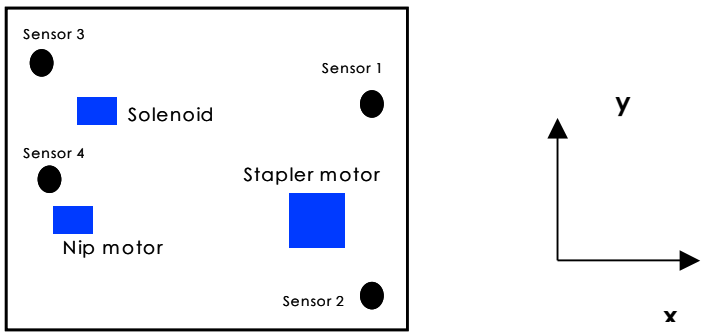

Figure 3: Top view of the finisher with location of the vibration sensors.

representation of the times the parts were on and the times the measurements were taken is given in Figure 2.

Although both sound and vibrations were measured in the experiment, we shall only analyze the vibration signals in this paper. In many industrial and office settings there is much background noise, making on-line monitoring of the machine using sound signals practically impossible. Hence, the vibration measurements appear to be the most promising for practical use. The vibrations were measured using four acceleration sensors located at four different positions in the finisher, see Figure 3. Each sensor measured vibrations in three orthogonal directions, converting the physical acceleration into voltage (V), with a sensitivity of 10 mV/g.

Before the experiment, a Failure Mode and Effect Analysis (FMEA) was performed in order to determine which internal parameters may have influence on the vibration pattern. The following seven were found: (i) Supply voltage 1, the voltage supplied to the motors and the solenoid, (ii) the stapler set size which is the number of sheets stapled, (iii) feed roll load, which measures the load on the feed roll and has direct influence on the nip transport motor, (iv) PWBA modification, (v) PWBA temperature, (vi) the tension of the belt which is located around the transport nip, and (vii) Supply voltage 2, the voltage supplied to the printed wire board assembly (PWBA). The levels over which the factors were varied are given

Factor	Level 1	Level 2	Level 3
P_1: Supply voltage 1 (Volt DC)	22	24	26
P_2: Paper set size (number of sheets)	5	27	50
P_3: Feed roll load	0 (Low)	-	1 (High)
P_4: PWBA modification	0 (Mod1)	-	1 (Mod2)
P_5: PWBA temperature	20	40	60
P_6: Belt tension	0 (Low)	-	1 (High)
P_7: Supply voltage 2 (Volt DC)	4.5	5.0	5.5

Table 1: Factors and their settings varied in the experiment.

in Table 1. For the purpose of the numerical regression they were coded according to Table 2.

The FMEA further indicated that the following interactions are important:

1. Supply voltage 1 × Paper set size
2. Supply voltage 1 × Feed roll load
3. Supply voltage 1 × PWBA Modification
4. Supply voltage 1 × PWBA Temperature
5. Paper set size × PWBA Modification
6. Paper set size × Feed roll load
7. PWBA Modification× Feed roll load

An echelon design was made using 20 combinations of settings and which allowed these interactions to be estimated (see [6]). This is in fact the smallest experimental design able to account for these seven factors at required number of levels. With the current study we attempted to find out if there are internal parameters that are both indicative of performance of the machine and possibly to recover easily accessible vibrational patterns of the device. For that reason, it is surprising how well the proposed calibration methods work already with small training set and minimal experimental design we could supply. This makes application of the method for greater training sets and more extended experimental design very promising.

At each setting, five replications were done on the same machine. Because the experiment was done in only two days, these replications should yield very similar measurements. Thus, for each time point in total 100 vibration signals were obtained. The sampling rate for each measurement was 40960 Hz, and the measurement was performed for a duration of 0.5 second, i.e., 20480 measurements were taken.

Not all of these seven parameters are indicative for the potential machine failure. For example, paper set size (P_2) is a nuisance parameter, which influence the vibration pattern but has no clear connection to the potential failure. On the other hand, supply voltage 1 (P_1) seems to have a close connection to current state of the system. However, if the nuisance parameter has influence on the vibration pattern used in order to perform system monitoring, then it is required to separate its effect at the pattern analysis. Therefore, it is also important to be able to recover the nuisance parameters.

Factor	Level 1	Level 2	Level 3
P_1: Supply voltage 1	-1	0	1
P_2: Paper set size	5	27	50
P_3: Feed roll load	0	-	1
P_4: PWBA modification	0	-	1
P_5: PWBA temperature	-1	0	1
P_6: Belt tension	0	-	1
P_7: Supply voltage 2	-1	0	1

Table 2: Coded factors and their settings varied in the experiment.

3 Calculation of external parameters

The objective of this paper is to calibrate the signal with the internal machine parameters given in Figure 4. Since the signal from each vibration sensor contains huge numbers of readings, it needs to be compressed, that is, the most informative parameters concerning the internal machine parameters need to be extracted from the signals in order to make calibration possible. Such a function of the vibration signal will be called an *external parameter*. Below, we first describe which time point we consider, and then describe how appropriate external parameters can be obtained from the vibration signals at that time point.

We focus on the stapling operation and, more specifically, only the time interval t2 in Figure 2 is considered, when the solenoid and the nip motor are off. The reason for this choice is that the noise in the measured signal for the stapler motor is minimal at t2, and therefore t2 is the most suitable for testing the present methodology. For other time points, more complex techniques like blind source separation may need to be used. The vibration sensor closest to the stapler motor was used, which is sensor 2 in Figure 2, so that we can assume that noise is negligible. Therefore, complex techniques like blind source separation do not need to be used to purify the signal, though for more complex systems it may be necessary (see e.g. [**?**]). Each vibration sensor reads vibration in three directions showed in Figure 3. Figure 4 shows the plot of the vibration signal for run 1, replication 1, direction z. This plot is similar to plots of all the other measured signals. Two clear "bursts" of high vibration can be observed. The first peak is caused by the anvil being pressed down on the paper and the second is caused by the staple being pressed through the paper.

A signal consisting of the 20480 measurements in one of the directions is denoted by the vector $\mathbf{w}$. We define the first burst to be the first 8000 measurements $(w_1, \ldots, w_{8000})$, and the second one to be the remaining measurements $(w_{8001}, \ldots, w_{20480})$. We consider the nine external parameters given below to be informative with respect to the internal parameters given in Table 1. The first and second internal parameters are the maximum absolute values of the signal corresponding to the two bursts:

$$\begin{aligned} \theta_1(\mathbf{w}) &= \max_{i \in \{1,8000\}} |w_i|, \\ \theta_2(\mathbf{w}) &= \max_{i \in \{8001,20480\}} |w_i|. \end{aligned}$$

These may be interpreted as the peak energy level corresponding to the two stapling procedures. The third and fourth external parameters are the energy contained in the first and

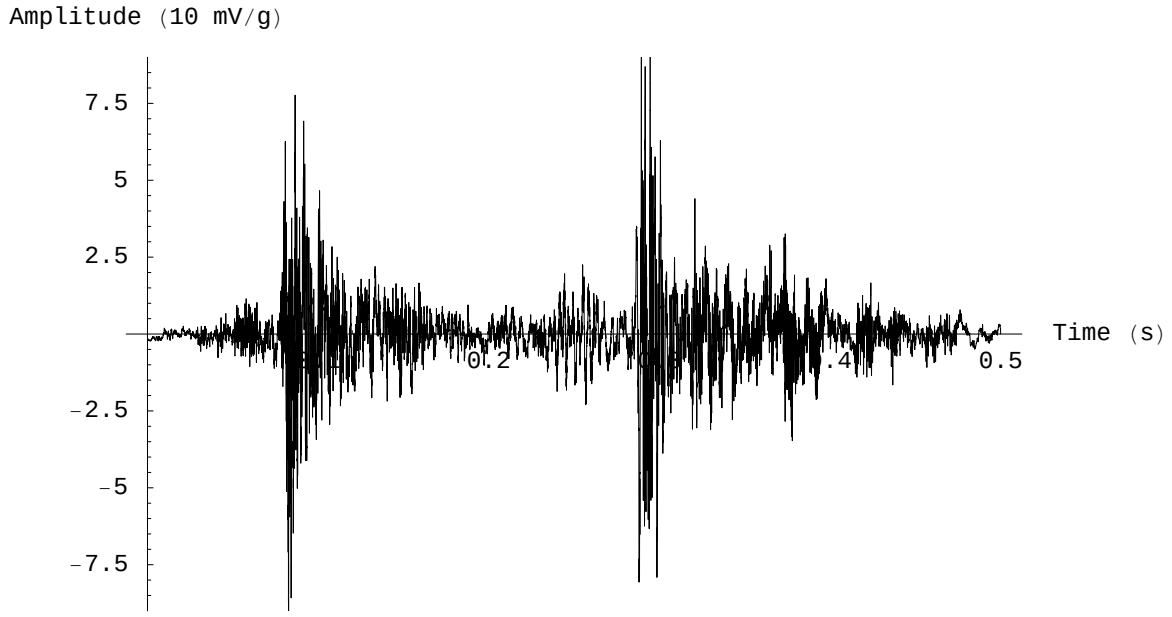

Figure 4: Vibration signal measured during the stapling process.

second bursts:

$$\begin{aligned}\theta_3(\mathbf{w}) &= 10^{-4} \sum_{i\in\{1,8000\}} w_i^2, \\ \theta_4(\mathbf{w}) &= 10^{-4} \sum_{i\in\{8001,20480\}} w_i^2.\end{aligned}$$

The fifth parameter is the distance between the peaks. Writing j_i for the index for which the ith burst occurs, it is given as

$$\theta_5(\mathbf{w}) = j_2 - j_1.$$

The parameters θ_1 to θ_5 have a clear physical interpretation. The following additional parameters, which do not have a clear physical interpretation, contain further important information. The sixth and seventh parameters are the average absolute values of the measurements:

$$\begin{aligned}\theta_6(\mathbf{w}) &= 10^{-4} \sum_{i\in\{1,8000\}} |w_i|, \\ \theta_7(\mathbf{w}) &= 10^{-4} \sum_{i\in\{8001,20480\}} |w_i|.\end{aligned}$$

The eighth and ninth are the fourth moments:

$$\begin{aligned}\theta_8(\mathbf{w}) &= 10^{-4} \sum_{i\in\{1,8000\}} w_i^4, \\ \theta_9(\mathbf{w}) &= 10^{-4} \sum_{i\in\{8001,20480\}} w_i^4.\end{aligned}$$

The parameters are calculated for the signals in all three directions, yielding 27 parameters in total.

In addition to the above, we have also looked at the power spectrum of the signals, but this did not seem to yield much additional information for the present purposes.

We denote by $\mathbf{w}_{ijk}$ ($i = 1, \ldots, 3$, $j = 1, \ldots, 20$ and $k = 1, \ldots, 5$) the measured signal for direction i, setting j, and replication k. Hence, for each setting j and replication k, we have a vector of 27 external parameters, given as

$$\mathbf{X}^T = (\theta_1(\mathbf{w}_{1jk}), \ldots, \theta_9(\mathbf{w}_{1jk}), \theta_1(\mathbf{w}_{2jk}), \ldots, \theta_9(\mathbf{w}_{2jk}), \theta_1(\mathbf{w}_{3jk}), \ldots, \theta_9(\mathbf{w}_{3jk})).$$

We hypothesize that these 27 external parameters contain most of the information in the vibration signal concerning the internal parameters P_1 to P_7 which were varied in the experiment (see Table 1). In the next section, we shall investigate to what extent this is true, that is, we shall try to calibrate these with the internal parameters. For notational simplicity we shall denote the (random) external parameters obtained from the signals by $\mathbf{X}^T = (X_1 \ldots, X_{27})$.

4 Calibration

Under calibration we will understand recovering real values of (some of) the internal parameters $P_1, \ldots, P_7$ given the value of corresponding observable values $X_1, \ldots, X_{27}$. In this section we will construct two possible calibration procedures using the *forward*, commonly used approach, and the *reverse* approach. For more details we refer to [**?**] and [7].

Most publications in this area are concerned with the *static* calibration problem such as determination of the concentration of various elements in a solution. For that purpose one may use spectral analysis or consider the electric properties of the solution. The problem we consider is somewhat different. It may be impossible to recover the internal parameters of the system using only one reading of the vibration. On the other hand, the vibration pattern contains a lot of information about the system. Therefore, as suggested, we need to perform a *dynamic* calibration. Moreover, it is not feasible to determine the vibrational pattern on the basis of physical laws since even simplest vibrating units are rather complicated systems.

First we separate the data into a *training* and a *validation* set where the training set will be used in order to construct the calibration procedure and the validation set in order to validate the procedure constructed. We assume that the data in the validation data set shows certain dependencies between observable values $X_1, \ldots, X_{27}$ separated in section 3 and internal parameters $P_1, \ldots, P_7$ in Table 2, but these dependencies are assumed to be additively disturbed by some random mechanism. For the validation data set we assume the same dependencies and the same kind of disturbance but this time independent from that for the training data set. Therefore, if the procedure constructed for the training data set is correct, it should work correctly for the validation data set. If it is not correct then, the constructed procedure is probably capturing random fluctuations of the training data as the expected dependencies and bases its conclusion on them.

On the other hand, correctness of the procedure for the training data set itself is also expected. Moreover, this procedure should work for the training data set even better than for the validation data set. This is because the training data set is already used for construction of the calibration procedure, so that random fluctuations are partly accounted for in the calibration procedure constructed.

Then we will separate the set of internal parameters between $P_1, \ldots, P_7$ which can be recovered by the methods of the calibration. Certainly, if any dependence between some P_k and the observable values $X_1, \ldots, X_{27}$ is missing, it is not possible to recover its value on the basis of $X_1, \ldots, X_{27}$. On the other hand, strict linear dependence without any random fluctuations guarantees successful calibration. Any situation between these two makes calibration possible. However, three questions are important, namely how complicated the relation is, how much it explains the variation in P_k, and how certain can we be about the presence of such a relation.

To discover complicated dependence between P_k and $X_1, \ldots, X_{27}$ much more data is required than for a simple dependence. In the current paper we only have at our disposal the results of 100 runs and for that reason we have to restrict ourselves to consideration of quadratic regressions. The second and third questions above will be answered by application of well-known statistical procedures.

Principal component analysis (PCA) is an important part of this and later analysis. It allows separation of uncorrelated factors from the data. It is also very important for the forward calibration approach.

The first calibration approach considered is the *forward* one. For this we regress internal parameters on the orthogonalized vectors of the observable values and consider this regression function as a predictor for the cases when the values of P_k are unknown. The second calibration approach considered is the *reverse* approach. It requires regression of the orthogonalized vectors of the observable values on the vectors of internal parameters and further reversion of this relation by means of minimal quadratic distance in order to predict the internal parameters when P_k is unknown.

The situation when P_k can take values only in some set $\mathcal{P}_k$ will be considered too. For the forward approach it requires minimization of a certain distance between prediction for $\mathbb{R}$ and prediction for $\mathcal{P}_k$. For the reverse approach it simply calls for minimization over $\mathcal{P}_k$ at reversion.

For both approaches we will check how close their values are to the observed ones in the Euclidian metric. Moreover, we will construct a restriction of these calibration methods to the set of all possible P_k and consider accuracy of calibration in terms of correct/incorrect calibration. For such restrictions it is possible to make a second choice and consider "best but one" candidate between all P_k. Their relative likelihood is a possible measure of certainty of the calibration. Larger ratio shows that the method does not hesitate between two possibilities. We will also consider in how many cases both first and second candidate were incorrect.

Finally, we will study how stable both calibration methods are related to the sample size. For this we will interchange the training and the validation data sets and repeat the same procedure.

4.1 Separation of internal parameters.

First we shall separate the data into a training data set which will be used in order to construct the calibration procedure and a validation data set which will be used to verify its correctness. For simplicity, only one training set is used. The training data set

$$(a_{i,1}, \ldots, a_{i,27}),\ i = 1, \ldots, 80,$$

contains the data from the first four of each five runs for each experiment. Consequently, the validation data set

$$(b_{i,1}, \ldots, b_{i,27}),\ i = 1, \ldots, 20$$

contains the data from each fifth run of each experiment.

Moreover, we shall centralize and standardize both data sets by the same means and standard deviations. Let

$$d_{i,j} = (a_{i,j} - m_j)/s_j,\ i = 1, \ldots, 80,\ j = 1, \ldots, 27,$$

where

$$m_j = \frac{1}{80}\sum_{i=1}^{80} a_{i,j}, \qquad s_j^2 = \frac{1}{79}\sum_{i=1}^{80}(a_{i,j} - m_j)^2,\ j = 1, \ldots, 27,$$

and let

$$c_{ij} = (b_{i,j} - m_j)/s_j,\ i = 1, \ldots, 20,\ j = 1, \ldots, 27.$$

In fact, we have performed the same linear transformation to all the data in both the training and the validation data sets.

First we perform the principal component analysis (PCA) of the training data set. It will result in a set of loading vectors $\mathbf{l}_1, \ldots, \mathbf{l}_{27}$ and a set of score vectors $(\mathbf{s}_1, \ldots, \mathbf{s}_{27})$, for which

$$(\mathbf{s}_1, \ldots, \mathbf{s}_{27}) = (\mathbf{d}_1, \ldots, \mathbf{d}_{27})(\mathbf{l}_1, \ldots, \mathbf{l}_{27})$$

(here and later we write $\mathbf{d}_j = (d_{1,j}, \ldots, d_{80,j})^T$). Similarly, we introduce

$$(\mathbf{s}'_1, \ldots, \mathbf{s}'_{27}) = (\mathbf{c}_1, \ldots, \mathbf{c}_{27})(\mathbf{l}_1, \ldots, \mathbf{l}_{27}). \tag{1}$$

We will also call the score vectors $\mathbf{s}'_1, \ldots, \mathbf{s}'_{27}$ the predicted score vectors. For notational simplicity we will also denote $\mathbf{P}_1, \ldots, \mathbf{P}_7$ vectors corresponding to the training data set and $\mathbf{P}'_1, \ldots, \mathbf{P}'_7$ vectors corresponding to the validation data set. Their meanings are described in Table 2.

First we use PCA in order to determine the set of parameters that can be recovered by the calibration using $X_1, \ldots, X_{27}$. For that we regress seven vectors $\mathbf{P}_1, \ldots, \mathbf{P}_7$ corresponding to different internal parameters linearly on $\mathbf{s}_1, \ldots, \mathbf{s}_{27}$ and the intercept.

$$\mathbf{P}_k = (\mathbf{1}, \mathbf{s}_1, \ldots, \mathbf{s}_{27})\mathbf{c}_k + \varepsilon_k,$$

where $\varepsilon_{\mathbf{k}} \sim \mathcal{N}(0, \mathbf{I}_{80}\sigma_k^2)$ are vectors of normal errors.

We only regress parameters $\mathbf{P}_k$ on linear terms since higher order regression would require estimation of 757 regression coefficients. They can not be solved from 80 equations. Though, application of the second order regression could make sense if we had very large data set.

Parameter	Name	R^2	p_F
P_1	Supply voltage 1	0.873	0.000
P_2	Paper set size	0.973	0.000
P_3	Feed roll load	0.281	0.785
P_4	PWBA modification	0.542	0.005
P_5	PWBA temperature	0.347	0.458
P_6	Belt tension	0.380	0.267
P_7	Supply voltage 2	0.274	0.815

Table 3: Regression of P_k - multiple R-squared statistic and p-value of multiple F-statistic.

When the first order regression captures dependence of parameter $\mathbf{P}_k$ on the scores, it is clear that this $\mathbf{P}_k$ is partly characterized by the observable variables. Moreover, when more variance in parameter $\mathbf{P}_k$ is explained, then $\mathbf{P}'_k$ can be recovered more accurately. In Table 4.1 we give the values of two statistics, the multiple R-squared statistic, and the p-value of the multiple F-statistic calculated for seven first order regressions.

Let us consider, for example, the internal parameter P_4. The value of its multiple R-squared statistic is 0.542. Therefore, regression explains approximately a half of its variation. It is better than for example for P_3 but still dependence of the parameter P_4 on the scores is weak compared to these for P_1 or P_2. The value of p_F is equal to 0.005. Therefore, effect of external parameters on P_4 is significant.

Analysis of this table suggests that it is possible to recover the values of internal parameters P_1, P_2, and P_4 using the separated data, whereas it is questionable whether it is possible for the other four internal parameters. Nevertheless, in the current paper we will restrict ourselves to recovering parameters P_1 and P_2 that depend on the extracted data most distinctly. They not only depend on the observed variables, but also larger part of their variance is explained by such dependence. As we will see later, P_1 is recovered less accurately than P_2 which is explained by the smaller multiple R-squared statistic.

4.2 Forward calibration.

First consider the forward calibration approach which is commonly used in the literature (see e.g. [7] and [?]). We regress parameters $\mathbf{P}_1$ and $\mathbf{P}_2$ on $\mathbf{s}_1, \ldots, \mathbf{s}_{27}$. Regressing up to the second order terms we found that only scores $\mathbf{s}_1, \ldots, \mathbf{s}_5$ are significant. We have selected terms

$$\mathbf{1},\ \mathbf{s}_1,\ \mathbf{s}_2\ ,\mathbf{s}_3\ ,\mathbf{s}_4\ ,\mathbf{s}_5\ ,\mathbf{s}_1^2\ ,\mathbf{s}_2^2\ ,\mathbf{s}_4^2\ ,\mathbf{s}_1\mathbf{s}_2\ ,\mathbf{s}_1\mathbf{s}_3\ ,\mathbf{s}_4\mathbf{s}_5$$

as significant for regression of parameters $\mathbf{P}_1$ and $\mathbf{P}_2$ on the scores. Here under product like $\mathbf{s}_1\mathbf{s}_2$ we understand a vector of componentwise products.

Let us denote the regression functions

$$\mathbf{P}_{i,k} = g_k(\mathbf{s}_{i,1}, \ldots, \mathbf{s}_{i,5}) + \varepsilon_{i,k},\ i = 1, \ldots, 80,\ k = 1, 2,$$

where

$$\varepsilon_{i,k} \sim \mathcal{N}(0, \sigma_k^2)$$

are independent normally distributed random errors, and $\mathbf{P}_{i,k}$ denotes the i-th component of the vector $\mathbf{P}_k$. Therefore, we also assume that

$$\mathbf{P}'_{i,k} = g_k(\mathbf{s}'_{i,1}, \ldots, \mathbf{s}'_{i,5}) + \varepsilon'_{i,k},\ i = 1, \ldots, 20,\ k = 1, 2,$$

where

$$\varepsilon'_{i,k} \sim \mathcal{N}(0, \sigma_k^2)$$

are independent normally distributed random errors.

Let for $(y_1, \ldots, y_5) \in \mathbb{R}^5$

$$(\hat{P}_1, \hat{P}_2) = (g_1(y_1, \ldots, y_5), g_2(y_1, \ldots, y_5)). \tag{2}$$

When considering possible values of (P_1, P_2) in $\mathbb{R}^2$, (2) provides a closed form solution for the calibration problem. In that form it can be directly applied to some vector $(x_1, \ldots, x_{27}) \in \mathbb{R}^{27}$ assumed to be the values extracted as described in section 3. That vector must be transformed according to (1) and then first five of its components must be substituted into (2).

As promised we apply (2) to the training and the validation data sets. Accuracy of the forward approach is pictured by the differences of vectors $\hat{\mathbf{P}}_1 - \mathbf{P}_1$, and $\hat{\mathbf{P}}'_1 - \mathbf{P}'_1$ (box plots 1 and 2 in Figure 7), and $\hat{\mathbf{P}}_2 - \mathbf{P}_2$, and $\hat{\mathbf{P}}'_2 - \mathbf{P}'_2$ (box plots 1 and 2 in Figure 8).

However, if the set of all possible values of $(P_1, P_2) \in \mathcal{P}_1 \times \mathcal{P}_2$ is known in advance, it is preferable to have $(\hat{P}_1, \hat{P}_2)$ lying in this set. For that, consider the following squared distance between $(\hat{P}_1, \hat{P}_2)$ in (2) and some $(P_1, P_2) \in \mathbb{R}^2$

$$\rho((P_1 - \hat{P}_1), (P_2 - \hat{P}_2)) = \hat{\sigma}_{P_1}^{-2}(P_1 - \hat{P}_1)^2 + \hat{\sigma}_{P_2}^{-2}(P_2 - \hat{P}_2)^2,$$

where σ_{P_1} and σ_{P_2} are estimated using the training data set only. It is proportional to minus the loglikelihood of (P_1, P_2) in the estimated model and it should be as small as possible.

Let

$$(\tilde{P}_1^1, \tilde{P}_2^1) = \text{argmin } \rho(P_1 - g_1(y_1, \ldots, y_5), P_2 - g_2(y_1, \ldots, y_5)), \tag{3}$$

where argmin is taken over the set $\mathcal{P}_1 \times \mathcal{P}_2$. This is another calibration mechanism, which also can be applied to any vector $(x_1, \ldots, x_{27}) \in \mathbb{R}^{27}$ assumed to be the values extracted as described in section 3.

We apply calibration method (3) to the training and the validation data set with $\mathcal{P}_1 \times \mathcal{P}_2 = \{-1, 0, 1\} \times \{5, 27, 50\}$ (choice of $\mathcal{P}_1 \times \mathcal{P}_2$ is explained in section 3). Numbers of cases for the training and for the validation data sets where the calibration by (3) did not recover the correct values of (P_1, P_2) are given in Table 4.

One can also look at the second candidate by the calibration procedure (3), namely

$$(\tilde{P}_1^2, \tilde{P}_2^2) = \text{argmin } \rho(P_1 - g_1(y_1, \ldots, y_5), P_2 - g_2(y_1, \ldots, y_5)), \tag{4}$$

where argmin is taken over the set $\mathcal{P}_1 \times \mathcal{P}_2 \setminus (\tilde{P}_1^1, \tilde{P}_2^1)$, and where $(\tilde{P}_1^1, \tilde{P}_2^1)$ is the same as in (3).

When the calibration is performed in order to define if the internal parameters are not in a critical set, it is advisable to look at the second candidate too. If the undesirable state is not $(\tilde{P}_1^1, \tilde{P}_2^1)$ but $(\tilde{P}_1^2, \tilde{P}_2^2)$, then it may be still advisable to monitor the system closely. The numbers of cases when both the first and the second choices were not correct can be found in Table 4.

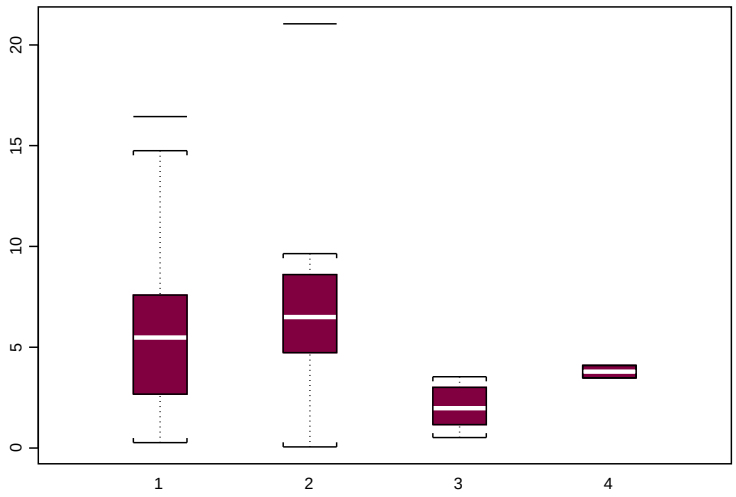

Figure 5: Forward approach - κ for training/validation sets, correct/incorrect calibration.

Moreover, the value of

$$\kappa = \rho(\hat{P}_1 - \tilde{P}_1^2, \hat{P}_2 - \tilde{P}_2^2) - \rho(\hat{P}_2 - \tilde{P}_2^1, \hat{P}_2 - \tilde{P}_2^1)$$

is proportional to the logarithm of the likelihood ratio of the first/second choice in the estimated model. When κ is large, then the probability of correct calibration by $(\tilde{P}_1^1, \tilde{P}_2^1)$ is higher. Box plots of the values of κ for the training data set, correct calibration (box plot 1), validation data set, correct calibration (box plot 2), training data set, incorrect calibration (box plot 3), and validation data set, incorrect calibration (box plot 4), are given on Figure 5.

From Figure 5 we conclude that the value of κ is informative as an indicator of certainty or uncertainty of the calibration though it is not able to indicate all incorrect calibrations without giving false alarm in case of correct calibrations.

4.3 Reverse calibration.

Anther approach to the calibration problem that we consider is the reverse calibration. We regress each of the scores $\mathbf{s}_1, \ldots, \mathbf{s}_{27}$ on the values of the parameters $(\mathbf{P}_1, \mathbf{P}_2)$ up to the second order terms. We have selected terms

$$\mathbf{1}, \mathbf{P}_1, \mathbf{P}_2, \mathbf{P}_1^2, \mathbf{P}_1\mathbf{P}_2$$

as significant for regression of the scores on the parameters $\mathbf{P}_1$ and $\mathbf{P}_2$. Unfortunately, the echelon minimal experimental design able to account for all seven factors with required number of levels which we have used does not allow to consider the dependent variable $\mathbf{P}_2^2$ too. We preferred $\mathbf{P}_1^2$ and $\mathbf{P}_1\mathbf{P}_2$ for two reasons. First, we would like to capture possible interaction between P_1 and P_2, and secondly, the value of the multiple R-squared statistic in Table 4.1 makes us think that P_1 may be more difficult to recover and hence, more precision in that direction is preferable. Let us denote the regression functions as

$$\mathbf{s}_{i,j} = f_j(\mathbf{P}_{i,1}, \mathbf{P}_{i,2}) + \varepsilon_{i,j}, \;\; i = 1, \ldots, 80, \;\; j = 1, \ldots, 27,$$

where

$$\varepsilon_{i,j} \sim \mathcal{N}(0, \sigma_j^2)$$

are independent normally distributed random errors.

Therefore we also assume that

$$\mathbf{s}'_{i,j} = f_j(\mathbf{P}'_{i,1}, \mathbf{P}'_{i,2}) + \varepsilon'_{i,j},\ i = 1, \ldots, 20,\ j = 1, \ldots, 27.$$

where

$$\varepsilon'_{i,j} \sim \mathcal{N}(0, \sigma_j^2)$$

are independent normally distributed random errors.

Let

$$(\hat{P}_1, \hat{P}_2) = \operatorname{argmin} \sum_{j=1}^{27} \left(y_j - f_j(P_1, P_2)\right)^2 / \hat{\sigma}_j^2, \tag{5}$$

where we minimize over $\mathbb{R}^2$, and where we have used only the training data set in order to estimate $\sigma_1, \ldots, \sigma_{27}$. In fact, that is approximate inversion of all regressions together. This is a calibration method that we will further call a forward calibration approach.

When considering possible values of (P_1, P_2) in $\mathbb{R}^2$, (5) provides a solution for the calibration problem. It can be directly applied to some vector $(x_1, \ldots, x_{27}) \in \mathbb{R}^{27}$ assumed to be the values extracted as described in section 3. That vector must be transformed according to (1) and then substituted into (5).

We also apply (5) to the training and the validation data sets. Accuracy of the reverse approach is pictured by the differences $\hat{\mathbf{P}}_1 - \mathbf{P}_1$, and $\hat{\mathbf{P}}'_1 - \mathbf{P}'_1$ (box plots 3 and 4 in Figure 7), and $\hat{\mathbf{P}}_2 - \mathbf{P}_2$, and $\hat{\mathbf{P}}'_2 - \mathbf{P}'_2$ (box plots 3 and 4 in Figure 8).

Application of all scores in the method is reasonable since the scores are uncorrelated (predicted scores - approximately uncorrelated) and the information about (P_1, P_2) contained in each of the scores is approximately independent. In fact, that is one of the advantages of the reverse calibration since for small training data sets the forward method can only use the most informative scores.

However, if the set of all possible values of $(P_1, P_2) \in \mathcal{P}_1 \times \mathcal{P}_2$ is known in advance, it is preferable to have $(\hat{P}_1, \hat{P}_2)$ lying in this set. For that, let

$$(\tilde{P}_1^1, \tilde{P}_2^1) = \operatorname{argmin} \sum_{j=1}^{27} \left(y_j - f_j(P_1, P_2)\right)^2 / \hat{\sigma}_j^2, \tag{6}$$

where we minimize over $\mathcal{P}_1 \times \mathcal{P}_2$.

We apply calibration method (6) to the training and the validation data set with $\mathcal{P}_1 \times \mathcal{P}_2 = \{-1, 0, 1\} \times \{5, 27, 50\}$. Numbers of cases for the training and for the validation data sets where the calibration by (6) did not recover correct values of (P_1, P_2) are given in Table 4.

One can also look at the second candidate by the calibration procedure (6), namely

$$(\tilde{P}_1, \tilde{P}_2) = \operatorname{argmin} \sum_{j=1}^{27} \left(y_j - f_j(P_1, P_2)\right)^2 / \hat{\sigma}_j^2, \tag{7}$$

where we minimize over $\mathcal{P}_1 \times \mathcal{P}_2 \setminus (\tilde{P}_1^1, \tilde{P}_2^1)$, and where $(\tilde{P}_1^1, \tilde{P}_2^1)$ is the same as in (6). The numbers of cases when both the first and the second choices were not correct can be found in Table 4.

Type of calibration	Training	Validation
Forward, first choice	10/80	2/20
Forward first & second choice	0/80	0/20
Reverse, first choice	2/80	0/20
Reverse, first & second choice	1/80	0/20
Reverse, first choice, small training set	5/80	0/20
Reverse, first & second choice, small training set	2/80	0/20

Table 4: Calibration errors.

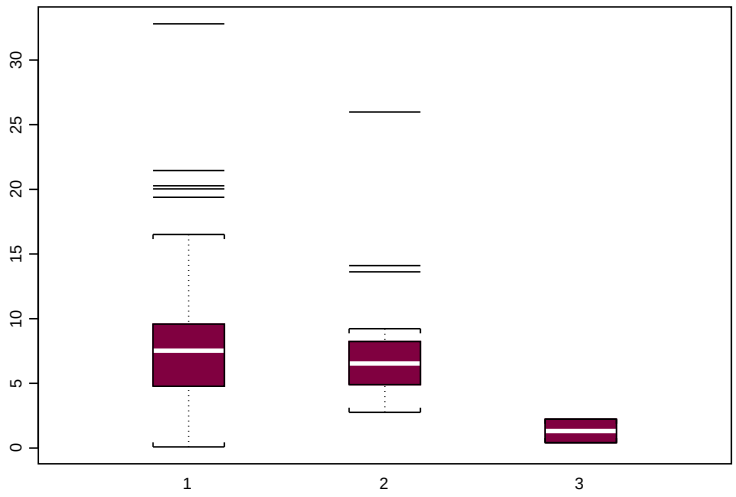

Figure 6: Reverse approach - κ for training/validation data set, correct/incorrect calibration.

Moreover, the value of

$$\kappa = \sum_{j=1}^{27} \left(y_j - f_j(\tilde{P}_1^2, \tilde{P}_2^2) \right)^2 / \hat{\sigma}_j^2 - \sum_{j=1}^{27} \left(y_j - f_j(\tilde{P}_1^1, \tilde{P}_2^1) \right)^2 / \hat{\sigma}_j^2$$

is proportional to the logarithm of the likelihood ratio of the first/second choice in the estimated model. When κ is large, then probability of correct calibration by $(\tilde{P}_1^1, \tilde{P}_2^1)$ is higher. Box plots of the values of κ for the training data set, correct calibration (box plot 1), validation data set, correct calibration (box plot 2), training data set, incorrect calibration (box plot 3), are given on Figure 6. The fourth box plot is missing since the reverse calibration does not calibrate incorrectly for the validation data set.

From Figure 6 we conclude that the value of κ is informative as an indicator of certainty or uncertainty of the calibration though it is not able to indicate all incorrect calibrations without giving false alarm in case of correct calibrations.

Moreover, we consider the reverse calibration approach only using first 18 of the presumably the most informative scores. Numbers of cases for the training and for the validation data sets where this calibration did not recover correct values of (P_1, P_2) and where both the first and the second choice by this calibration were not correct can be found in Table 4.

Type of calibration	Training	Validation
Forward, first choice	34/80	0/20
Forward first & second choice	19/80	0/20
Reverse, first choice	16/80	0/20
Reverse, first & second choice	4/80	0/20

Table 5: Calibration errors, interchanged roles.

4.4 Smaller training data set.

It also makes sense to check how stable both methods are with respect to the sample size. For that we interchange the roles of the training and the validation data sets and performed the same analysis. It is summarized in Table 5.

It appeared that already for this small training data set size accuracy of the calibration algorithms is quite high. Nevertheless, it is still desirable to provide a large training data set in order to reach better calibration algorithm. Also, the reverse calibration is found to be more accurate already for a small training data set.

4.5 Comparison of both calibration methods

Tables 4 and 5 suggest that the reverse approach is preferable to the forward one since its accuracy is much higher, though in one case it fails to detect the correct value of (P_1, P_2) by both the first and the second choice. The forward approach never misses the correct value of the pair by both the first and the second choices.

Moreover, it is interesting how much the reverse approach uses the observed data. So, if we would only consider regression of the first 18 scores on the values of P_1 and P_2, then the reverse approach would also make more calibration errors. Therefore, the reverse calibration approach is more suitable for the purpose of dynamic calibration where the signal in time domain can be compressed into high-dimensional vector (in the current study, its dimension is equal to 27 as we discussed in section 4).

Reverse calibration is also less dependent on the PCA analysis. It only uses it in order to determine which of P_k can be recovered by the calibration and orthogonalize vectors of dependent variables.

Figures 7 shows that precision of the forward calibration of P_1 in the continuous metric is also lower whereas for P_2 they both are approximately equally good. It may be explained by the fact that calibration of P_2 is more accurate.

All analysis in this section were performed using S-PLUS. S-PLUS code for calibration functions and all used data are available from the first author.

In principle, it is also possible to use estimates of the form

$$(P_1, P_2) = \operatorname{argmin} \sum_{j=1}^{27} h\left(\left(y_j - f_j(P_1, P_2)\right)/\hat{\sigma}_j\right),$$

where h is some monotone increasing function e.g. $h_z(x) = 1\{x \le z\}$ or $h(x) = |x|$. The first one can be extremely helpful if the considered regression only explains a part of the variation in the parameters P_1 and P_2. However, the calibration problem considered in the current paper is solved more efficiently by setting $h(x) = x^2$. Also, it provides a likelihood ratio related predictor of accuracy of the calibration performed.

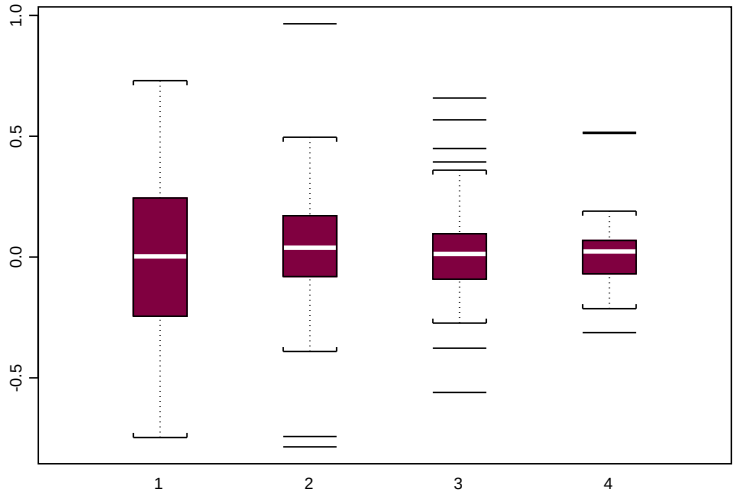

Figure 7: P_1 errors, forward/reverse, training/validation.

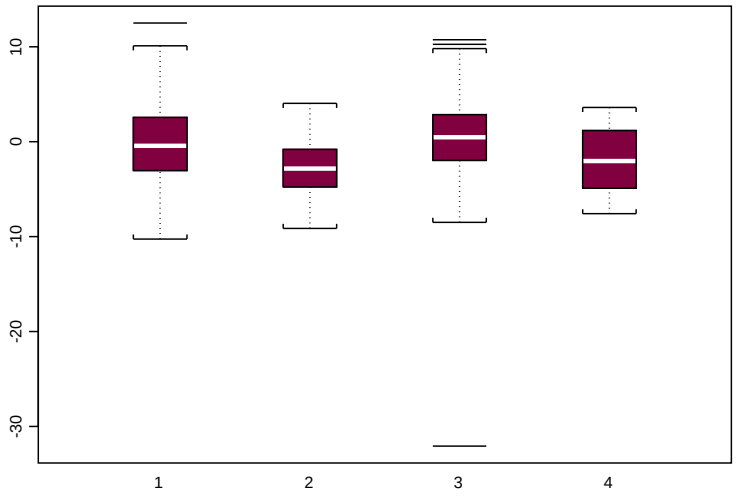

Figure 8: P_2 errors, forward/reverse, training/validation.

5 Conclusion and Discussion

Today there is a need for cheap practical methods for the purposes of online monitoring of machine performance and for the assessment of the remaining life-time of components. A potentially promising signal to measure in this respect is the vibration produced by a component. If the accelerometer is placed close to the relevant component, a relatively clean signal may be obtained. The aim of this paper is to investigate whether indeed vibrations can be used for these purposes, and if so to present a practical methodology by which this can be done. The results of this paper show that the answer to the question is affirmative. Furthermore, practical dynamic calibration methods were presented for decoding the aggregated profile represented by the machine's vibrations. Note that the purpose of this paper was not to present a completely thorough analysis of the copying machines under investigation, but rather to show that the general methodology is practical, which has been done successfully.

In the current paper we have investigated two calibration methods, namely the forward and reverse ones. It is clear that the reverse calibration is preferable for the experiment considered. One of its strong sides is that it is able to use all the data contained in the observations in a more efficient way than the forward calibration which is restricted to the use of some of the first scores, explaining most of the variation in the observations. This makes the reverse approach more suitable for dynamic calibration. Its advantage can also be seen from comparison of the reverse calibration procedures using only the first 18 scores to the reverse calibration procedure using all scores and its quality for smaller training data sets. One immediately striking advantage of the forward calibration is its computational simplicity when maximizing over large set of possible values of (P_1, P_2), though when the set of possible values of the internal parameters is restricted this advantage is minimal.

In order to apply the calibration procedures developed in this paper for the assessment of the remaining life-time of components and for online monitoring, a more elaborate experiment should be done than the experiment presented in the current paper, which was a screening experiment. In particular, more settings of the internal parameters should be used, and preferably multiple machines should be tested. In future research we also suggest to consider other types of the signal compression. For example, instead of looking for physically interpretable compression it may be interesting to look at wavelet coefficients of the vibrational signal.

Acknowledgements: The authors wish to thank Dr. A. Di Bucchianico and Prof. H. Wynn for their fruitful suggestions and comments.

Author's biographies

Vladimir Kulikov (kulikov 'at' eurandom.tue.nl) received his PhD in statistics from the Delft University of Technology, the Netherlands in January 2003. He is currently research fellow at EURANDOM, the Netherlands. His main research interests are maximum likelihood estimation, estimation under constraints, two samples testing, and calibration.

Wicher Bergsma (bergsma 'at' eurandom.tue.nl) is research fellow at EURANDOM in Eindhoven, the Netherlands. His research interests include categorical data analysis, nonparametric (multivariate) statistics, industrial statistics and numerical optimization. He has

	P_1	P_2
Intercept	-0.554	20.094
s_1	0.055	-5.441
s_2	-0.002	0.086
s_3	0.278	1.792
s_4	0.004	-2.737
s_5	-0.176	2.802
s_1^2	0.042	0.533
s_2^2	0.034	0.403
s_5^2	-0.105	-1.120
$s_1 s_2$	-0.045	-0.395
$s_1 s_3$	-0.053	-0.182
$s_4 s_5$	0.138	0.513
StDev	0.373	4.69

Table 6: Forward approach - regression coefficients.

had previous appointments at Tilburg University and the Central European University in Budapest.

References

[1] W J Wang and P D McFadden. Application of wavelets to gearbox vibration signals for fault detection. *Journal of Sound and Vibration*, 192(5):927–939, 1996.

[2] P W Tse, Y H Peng, and R Yam. Wavelet analysis and envelope detection for rolling element bearing fault diagnosis. *Journal of Vibration and Acoustics*, 123:303–310, 2001.

[3] G G Yen and K K Lin. Wavelet packet feature extraction for vibration monitoring. *IEEE Trans on Industrial Electronics*, 47(3):650–667, 2000.

[4] K Mori, N Kasashima, T Yoshioka, and Y Ueno. Prediction of spalling on a ball bearing by applying the discrete wavelet transform to vibration signals. *Wear*, 195:162–168, 1996.

[5] T. Figarella. Signature analysis: Modelling the characteristics of the main tray of the Lake finishers. Master's thesis, Eindhoven University of Technology, Eindhoven, 2003.

[6] A Di Bucchianico and H P Wynn. Echelon designs: algebra and application. *Submitted*, pages 1–5, 2004.

[7] P J Brown. *Measurement, regression, and calibration*. Oxford, Clarandon Press, 1993.

6 Appendix

6.1 Tables of regression coefficients

In Tables 6 and 7 we provide regression coefficients and standard deviation used in the previous analysis.

	Intercept	P_1	P_2	P_1^2	P_1P_2	StDev
s_1	3.8299	2.6654	-0.1528	0.4732	-0.0458	1.1890
s_2	-3.7081	0.2025	0.0123	4.2209	0.0105	1.5960
s_3	-0.1856	0.9639	0.0163	-0.3774	0.0086	1.1080
s_4	0.7441	-0.7091	-0.0230	-0.1761	0.0088	1.2040
s_5	-0.3652	0.2976	0.0072	0.2165	-0.0172	0.7969
s_6	-0.3606	-0.2207	-0.0004	0.4540	0.0105	0.8060
s_7	0.4866	0.1483	0.0001	-0.6037	-0.0029	0.8060
s_8	-0.1339	0.2588	0.0012	0.1313	-0.0098	0.5102
s_9	-0.0705	-0.0733	-0.0007	0.0880	0.0046	0.5630
s_{10}	0.0416	-0.1440	-0.0003	-0.0426	0.0052	0.4591
s_{11}	0.0917	-0.1027	-0.0006	-0.0687	0.0038	0.4168
s_{12}	0.0707	0.1082	0.0011	-0.1202	-0.0024	0.3919
s_{13}	-0.0531	-0.1595	-0.0026	0.1378	0.0035	0.3809
s_{14}	-0.0863	0.0288	-0.0006	0.1089	-0.0006	0.3382
s_{15}	0.0317	-0.0687	-0.0013	0.0241	0.0020	0.3140
s_{16}	-0.0009	-0.0763	0.0000	-0.0046	0.0008	0.2893
s_{17}	0.0548	-0.0115	-0.0001	-0.0420	0.0002	0.2269
s_{18}	-0.0350	0.0243	0.0007	0.0118	-0.0005	0.1812
s_{19}	-0.0108	0.0405	0.0000	0.0246	-0.0012	0.1878
s_{20}	-0.0464	-0.0585	-0.0008	0.0754	0.0018	0.1548
s_{21}	-0.0478	0.0163	-0.0002	0.0605	-0.0004	0.1302
s_{22}	-0.0179	0.0110	-0.0001	0.0223	-0.0001	0.1056
s_{23}	0.0034	-0.0052	0.0000	-0.0014	0.0005	0.0985
s_{24}	0.0013	-0.0217	-0.0002	0.0067	0.0005	0.0814
s_{25}	0.0026	-0.0158	0.0001	-0.0073	0.0007	0.0660
s_{26}	0.0335	-0.0049	0.0000	-0.0366	0.0003	0.0366
s_{27}	0.0075	-0.0014	-0.0001	-0.0063	0.0001	0.0371

Table 7: Reverse approach - regression coefficients.

6.2 SPLUS code

Forward calibration, restricted set of possible values.
Requires vector **xx** of length 5 which consists of the first five score coordinates and matrix **a** of size 13×2 as described in Table 6.
Returns vector of length 5 containing first choice, second choice, and the value of κ.

```
   function(xx,a)
{
    x<-c(1,xx,xx[1]^2,xx[2]^2,xx[4]^2,xx[1]*xx[2],xx[1]*xx[3],xx[4]*xx[5])
    i<-1
    j<-1
    min<-1e+022
    prevmin<-1e+022
    ans<-c(-1e+022,-1e+022)
    prevans<-c(-1e+022,-1e+022)
    x1<-c(-1,0,1)
    x2<-c(5,27,50)
    for(i in 1:3){
        for(j in 1:3){
        dist<-(x%*%a[1:12,1]-x1[i])^2/a[13,1]^2+(x%*%a[1:12,2]-x2[j])^2/a[13,2]^2
            if(dist<min){
                min<-dist
                ans<-c(x1[i],x2[j])
            }
        }
    }
    for(i in 1:3){
        for(j in 1:3){
        dist<-(x%*%a[1:12,1]-x1[i])^2/a[13,1]^2+(x%*%a[1:12,2]-x2[j])^2/a[13,2]^2
            if(dist<prevmin & abs(dist-min)>1e-050){
                prevmin<-dist
                prevans<-c(x1[i],x2[j])
            }
        }
    }
    return(c(ans, prevans, prevmin-min))
}
```

Forward calibration, non-restricted set of possible values.
Requires vector **xx** of length 5 which consists of the first five score coordinates and matrix **a** of size 13×2 as described in Table 6.
Returns vector of length 2 containing the result of forward calibration.

```
   function(xx,a)
{
    x<-c(1,xx,xx[1]^2,xx[2]^2,xx[4]^2,xx[1]*xx[2],xx[1]*xx[3],xx[4]*xx[5])
              return(x%*%a[1:12,])
```

```
}
```

Reverse calibration, restricted set of possible values.
Requires vector x of length 27 which contains all score coordinates, matrix z of size 6x27 as described in Table 6, and vector **v** of length 27 which characterizes contribution of each score into calibration. In the paper choices $\mathbf{v} = (1, \ldots, 1)$ and $\mathbf{v} = (1, \ldots, 1, 0, \ldots, 0)$ are made, where zero's are on the last 9 places.
Returns vector of length 5 containing first choice, second choice, and the value of κ.

```
   function(x,z,v)
{
    i1<-1
    i2<-1
    i3<-1
    min<-(1e+022)
    min2<-(1e+022)
    argmin<-0
    argmin2<-0
    for(i1 in 1:3){
        for(i2 in 1:3){
                a<-c(1,i1-2,0,0,0)
                if(i2==1){
                    a[3]<-5
                }
                if(i2==2){
                    a[3]<-27
                }
                if(i2==3){
                    a[3]<-50
                }
                a[4]<-a[2]^2
                a[5]<-a[2]*a[3]
                b<-((a%*%z[1:5,]-x)^2/(z[6,]^2))+log(z[6,])
                s<-b%*%v
                if(min>s){
                    min<-s
                    argmin<-a
            }
        }
    }
    for(i1 in 1:3){
        for(i2 in 1:3){
                a<-c(1,i1-2,0,0,0)
                if(i2==1){
                    a[3]<-5
                }
```

```
                if(i2==2){
                    a[3]<-27
                }
                if(i2==3)){
                    a[3]<-50
                }
                a[4]<-a[2]^2
                a[5]<-a[2]*a[3]
                b <-((a%*%z[1:5,]-x)^2/(z[6,]^2))+log(z[6,])
                s<-b%*%v
                if(min2>s & nopp(argmin,a)){
                    min2<-s
                    argmin2<-a
                }
        }
    }
    return(c(argmin[2:3],argmin2[2:3],(min2-min)))
}
```

Where function *nopp* is given by

```
   function(x,y)       (nopp)
{
    i<-0
    flag<-F
    for(i in 1:length(x)){
        if(x[i]!=y[i]){
            flag<-T
        }
    }
    return(flag)
}
```

requires two vectors of equal length and returns "T" is they are not exactly the same.

Reverse calibration, non-restricted set of possible values.
This requires two functions: the first one takes care of minimization by means of SPLUS function nlminb. Requires vector **x1** of length 27 containing all score coordinates, matrix **z** of size 6×27 as described in Table 7, vector **v** of length 27 which characterizes contribution of each score into calibration, and the starting value **st** (it may be taken $(0, 0)$). In the paper choice $\mathbf{v} = (1, \ldots, 1)$ is made, where zero's are on the last 9 places.
Returns vector of length 2 containing minimizer of the function $Rev.non_restr()$ being result of the reverse calibration.

```
   function(x1,z1,v1,st)
{
```

```
    return(nlminb(start=st,objective=Rev.non_restr,x=x1,z=z1,v=v1)$parameters)
}
```

Requires vector **x** of length 27, matrix **z** of size 6×27, and vector **v** of length 27. In the paper $v = (1, \ldots, 1)$ is taken.
Returns the values of the quadratic sum.

```
   function(aa,x,z,v)        (Rev.non_restr)
{
    a<-c(1,aa,aa[1]^2,aa[1]*aa[2])
    b<-((a%*%z[1:5,]-x)^2/(z[6,]^2))
    s<-b%*%v
    return(s)
}
```

In our study all these functions were applied to calibration of two vectors $\mathbf{P1}'$, $\mathbf{P2}'$, and **P1**, **P2**. For this reason they were applied by the function

```
   function(x,y,v)
{
    i<-1
    a<-c(0,,0)
    for(i in 1:N){
        a<-rbind(a,CALIBRATION.FUNCTION(x[i,],y,v))
    }
    return(a[2:N+1,])
}
```

It requires matrix **x** of proper dimension (its rows will be used in each calibration procedure), matrix **y** is in Tables 6 or 7, and vector **v** if any.